

ACE2/Ang(1-7)/Mas轴对尿毒症大鼠高转化骨病的改善作用

薛 杨, 阮颖新, 闫铁昆, 贾俊亚, 林 珊
(天津医科大学总医院肾内科, 天津 300054)

[摘要] **目的:** 探讨血管紧张素(1-7) [Ang(1-7)] 对大鼠尿毒症高转性骨病的影响, 并阐明其可能的机制。**方法:** 30只SD大鼠随机分为假手术组($n=6$)和实验组($n=24$), 实验组大鼠采用5/6肾切除术(Platt法)+高磷(P)饮食[1.2% P, 1.0%钙(Ca)]制备尿毒症高转化骨病模型, 并将建模成功的大鼠随机分为模型组、Ang(1-7)组、血管紧张素转换酶2(ACE2)激活剂二乙酰胺三氮脒(DIZE)组(DIZE组)和Mas受体拮抗剂组(A779组), 每组6只。分别于手术后12和18周采用全自动生化分析仪检测各组大鼠血清Ca、P、血肌酐(Scr)、血尿素氮(BUN)和24h尿蛋白(UP)水平; 免疫化学荧光法测定各组大鼠全段甲状旁腺素(iPTH)水平; 酶联免疫吸附试验(ELISA)法检测各组大鼠血清骨钙素(OC)、I型胶原N端肽(NTX)和抗酒石酸酸性磷酸酶(TRAP)-5b水平; 高分辨率显微CT扫描检测各组大鼠股骨组织的骨密度(BMD)、组织骨密度(TMD)、骨小梁厚度(Tb.Th)和骨小梁分离度(Tb.Sp)等三维结构参数。Von Kossa染色和吉姆萨染色观察各组大鼠皮质骨及骨小梁病理形态表现, 计算骨小梁体积(TBV); 荧光显微镜下测定各组大鼠骨矿化率(MAR), 并计算成骨细胞指数(OBI)和破骨细胞指数(OCI)。**结果:** 术后12和18周, 与假手术组比较, 模型组、Ang(1-7)组、DIZE组和A779组大鼠体质量减小($P<0.05$); 术后12和18周, 与假手术组比较, 模型组、Ang(1-7)组、DIZE组和A779组大鼠血清中24h UP、Scr及BUN水平均升高($P<0.05$); 术后18周, 与模型组比较, Ang(1-7)组和DIZE组大鼠血清中24h UP及Scr水平均降低($P<0.05$), A779组大鼠血清中24h UP、Scr和BUN水平均升高($P<0.05$)。证实尿毒症高转化骨病大鼠模型构建成功。术后12和18周, 与假手术组比较, 模型组、Ang(1-7)组、DIZE组和A779组大鼠血清中iPTH、P、OC、NTX及TRAP-5b水平均升高($P<0.05$); 术后18周, 与模型组比较, Ang(1-7)组和DIZE组大鼠血清中NTX及TRAP-5b水平均降低($P<0.05$), A779组大鼠血清中iPTH、P、NTX和TRAP-5b水平均升高($P<0.05$)。高分辨率显微CT扫描检测, 与假手术组比较, 模型组、Ang(1-7)组、DIZE组和A779组大鼠股骨BMD及TMD均降低($P<0.05$); 与模型组比较, Ang(1-7)组和DIZE组大鼠股骨BMD及TMD均升高($P<0.05$), A779组大鼠股骨BMD和TMD均降低($P<0.05$)。与假手术组比较, 模型组大鼠股骨Tb.Th降低($P<0.05$), Tb.Sp升高($P<0.05$); Ang(1-7)组和DIZE组大鼠股骨Tb.Th升高($P<0.05$), 而Tb.Sp降低($P<0.05$); 与模型组比较, A779组大鼠股骨Tb.Th降低($P<0.05$), 而Tb.Sp升高($P<0.05$)。骨病理检查, 与假手术组比较, 模型组、Ang(1-7)组、DIZE组和A779组大鼠股骨TBV均降低($P<0.05$), MAR、OBI和OCI均升高($P<0.05$); 与模型组比较, Ang(1-7)组和DIZE组大鼠股骨OBI及OCI均降低($P<0.05$), TBV升高($P<0.05$), 而A779组大鼠股骨OBI和OCI均升高($P<0.05$), TBV降低($P<0.05$)。**结论:** ACE2/Ang(1-7)/Mas轴对尿毒症大鼠高转化骨病具有改善作用。

[收稿日期] 2023-10-31 [录用日期] 2024-03-19

[基金项目] 国家自然科学基金青年基金项目(82000669); 国家自然科学基金面上基金项目(81570630); 天津市医学重点学科(专科)建设项目(TJYXDJK-071C); 天津市卫健委科技项目(ZC20219)

[作者简介] 薛 杨(1980—), 女, 天津市人, 主治医师, 医学博士, 主要从事肾性骨病基础和临床方面的研究。

[通信作者] 林 珊, 主任医师, 教授, 博士研究生导师(E-mail: linshan1012@163.com);
贾俊亚, 主任医师, 教授, 硕士研究生导师(E-mail: youshalei@126.com)

[关键词] 尿毒症; 高转化骨病; 成骨细胞; 破骨细胞; 血管紧张素转换酶2; 血管紧张素(1-7)
[中图分类号] R563.13 [文献标志码] A

Ameliorative effect of ACE2/Ang(1-7)/Mas axis on high-turover bone disease in uremic rats

XUE Yang, RUAN Yingxin, YAN Tiekun, JIA Junya, LIN Shan

(Department of Nephrology, First Affiliated Hospital, Tianjin Medical University, Tianjin 300054, China)

ABSTRACT Objective: To discuss the effect of angiotensin (1-7) [Ang (1-7)] on high-turnover bone disease in the uremic rats, and to clarify its possible mechanism. **Methods:** Thirty SD rats were randomly divided into sham operation group ($n=6$) and experimental group ($n=24$). The rats in experimental group underwent 5/6 nephrectomy (Platt method) + high-phosphorus (P) diet [1.2% P, 1.0% calcium (Ca)] to establish the model of uremic high-turnover bone disease. The successfully modeled rats were then randomly divided into model group, Ang (1-7) group, angiotensin-converting enzyme 2 (ACE2) activator dimethylacetamide amidoxime (DIZE) group, and Mas receptor antagonist group (A779 group), with 6 rats in each group. The levels of Ca, P, blood creatinine (Scr), blood urea nitrogen (BUN), and 24 h urinary protein (UP) in serum of the rats in various groups were detected by automatic biochemical analyzer at 12 and 18 weeks after operation; immunofluorescence staining was used to detect the levels of intact parathyroid hormone (iPTH) in the rats in various groups; ELISA method was used to detect the levels of osteocalcin(OC), type I collagen N-terminal peptide (NTX), and tartrate-resistant acid phosphatase (TRAP)-5b in serum of the rats in various groups; high-resolution micro-CT scan was used to detect the bone density (BMD), tissue mineral density (TMD), trabecular thickness (Tb.Th), and trabecular separation (Tb.Sp) in femur tissue of the rats in various groups; Von Kossa staining and Giemsa staining were used to observe the pathomorphology of cortical bone and trabecular bone of the rats in various groups, and the trabecular bone volume (TBV) was calculated; fluorescence microscope was used to detect the mineral apposition rates (MAR) of the rats in various groups, and the osteoblast index (OBI) and osteoclast index (OCI) of the rats in various groups were calculated. **Results:** At 12 and 18 weeks after operation, compared with sham operation group, the weights of the rats in model group, Ang (1-7) group, DIZE group, and A779 group were decreased ($P<0.05$). At 12 and 18 weeks after operation, compared with sham operation group, the levels of 24 h UP, Scr, and BUN in serum of the rats in model group, Ang (1-7) group, DIZE group, and A779 group were increased ($P<0.05$); at 18 weeks after operation, compared with model group, the levels of 24 h UP and Scr in serum of the rats in Ang (1-7) group and DIZE group were decreased ($P<0.05$), and the levels of 24 h UP, Scr and BUN in serum of the rats in A779 group were increased ($P<0.05$). The successful establishment of the uremic high-turnover bone disease model was confirmed. At 12 and 18 weeks after operation, compared with sham operation group, the serum iPTH, P, OC, NTX, and TRAP-5b levels of the rats in model group, Ang (1-7) group, DIZE group, and A779 group were all significantly increased ($P<0.05$); at 18 weeks after operation, compared with model group, the serum NTX and TRAP-5b levels of the rats in Ang (1-7) group and DIZE group were decreased ($P<0.05$), while the serum iPTH, P, NTX and TRAP-5b levels in A779 group were increased ($P<0.05$). The high-resolution micro-CT scan results showed that compared with sham operation group, the values of femur BMD and TMD of the rats in model group, Ang (1-7) group, DIZE group, and A779 group were all significantly decreased ($P<0.05$); compared with model group, the values of femur BMD and TMD of the rats in Ang (1-7) group and DIZE group were increased ($P<$

0.05), while the values of BMD and TMD of the rats in A779 group were decreased ($P < 0.05$). Compared with sham operation group, the femur Tb. Th of the rats in model group was decreased ($P < 0.05$), and the Tb. Sp was increased ($P < 0.05$); the femur Tb. Th of the rats in Ang(1-7) group and DIZE group were increased ($P < 0.05$), and the Tb. Sp was decreased ($P < 0.05$). Compared with model group, the femur Tb. Th of the rats in A779 group was decreased ($P < 0.05$), and the Tb. Sp was increased ($P < 0.05$). The bone pathological examination results showed that compared with sham operation group, the femur TBV of the rats in model group, Ang(1-7) group, DIZZ group and A779 group were decreased ($P < 0.05$), and MAR, OBI and OCI were increased ($P < 0.05$); compared with model group, the OBI and OCI of the rats in Ang(1-7) group and DIZE group were decreased ($P < 0.05$), and TBV was increased ($P < 0.05$), while the OBI and OCI of the rats in A779 group were increased ($P < 0.05$), and TBV was decreased ($P < 0.05$). **Conclusion:** The ACE2/Ang (1-7)/Mas axis improves high-turnover bone disease in the uremic rats.

KEYWORDS Uremia; High-turnover bone disease; Osteoblasts; Osteoclasts; Angiotensin-converting enzyme 2; Angiotensin (1-7)

肾素-血管紧张素系统 (renin-angiotensin system, RAS) 由肾素、血管紧张素转换酶 (angiotensin-converting enzyme, ACE)、血管紧张素 II (angiotensin II, Ang II)、血管紧张素受体、血管紧张素 (1-7) [angiotensin 1-7, Ang (1-7)] 和 Mas 受体组成^[1]。研究^[2]表明: 局部组织 RAS 在骨代谢中起着关键作用, 这种作用独立于全身 RAS。RAS 在人类骨组织中也有表达^[3]。采用逆转录聚合酶链式反应 (reverse transcription-polymerase chain reaction, RT-PCR) 在人类骨髓样本中检测到 RAS 组分^[4]。成骨细胞和破骨细胞均能在体内及体外表达 ACE2 和 Mas 受体^[5]。通过激活 ACE2/Ang (1-7) /Mas 轴可以刺激成骨细胞增殖, 抑制破骨细胞活性, 从而降低骨吸收、促进骨重塑, 进而改善骨质疏松症状^[6]。在此过程中, Ang (1-7) 表现出抑制肾素活性, 并通过促进成骨因子表达和抑制破骨因子生成, 实现增加骨小梁数量、提升骨密度和骨机械强度的效果^[7]。研究^[8]显示: 慢性肾脏病矿物质和骨代谢异常 (chronic kidney disease-mineral and bone disorder, CKD-MBD) 中高转化骨病的发病机制与 RAS 系统的异常激活存在密切关联。在 CKD-MBD 患者体内, 由于肾脏功能受损, 肾素分泌增加, 导致 RAS 过度激活。这种过度激活的 RAS 通过促进破骨细胞活性和抑制成骨细胞增殖, 导致骨吸收增加和骨重塑障碍, 最终加剧高转化骨病的进展^[9]。本研究探讨 ACE2/Ang (1-7)/Mas 轴对尿毒症大鼠高转化骨病状态的影响, 阐明 ACE2/Ang (1-7)/Mas 轴在 CKD-MBD 高转化骨病的作用机制, 为

CKD-MBD 提供新的治疗思路和靶点。

1 材料与方法

1.1 实验动物、主要试剂和仪器 30只5周龄雄性 SD 大鼠购自斯贝福 (北京) 生物技术有限公司, 动物生产许可证号: SCXK (京) 2019-0010, 体质量 (150 ± 10)g, 饲养于天津医科大学实验动物中心。所有 SD 大鼠均饲养于 22°C 、12 h 光/暗循环的无特定病原体级标准动物房中, 自由摄取食物和饮水; 本研究动物方案经本院伦理委员会审核通过, 所有动物操作均符合实验动物使用和保护条例。实验用 Ang (1-7) 购自上海恒渡生物科技有限公司, 二乙酰胺三氮脒 (diminazene aceturate, DIZE) 标准品购自上海甄准生物科技有限公司, Ang (1-7) 受体 Mas 抑制剂 A779 购自北京百奥莱博科技有限公司, 小鼠抗酒石酸酸性磷酸酶 (tartrate-resistant acid phosphatase, TRAP)-5b 酶联免疫吸附试验 (enzyme-linked immunosorbent assay, ELISA) 试剂盒购自上海恪敏生物科技有限公司, 小鼠 I 型胶原 N 端肽 (N-telopeptide of type I collagen, NTX) ELISA 试剂盒购自南京森贝伽生物科技有限公司, 骨钙素 (osteocalcin, OC) ELISA 检测试剂盒购自上海西唐生物科技有限公司, 注射用盐酸四环素购自上海新亚药业有限公司。皮下微量注射泵购自美国 Harvard Apparatus 公司, 高分辨率显微 CT 和高分辨率 231Micro VIVA-CT80 系统均购自瑞士 Scanco 医疗股份公司, 荧光显微镜、全自动图像数字化分析仪和轮转式切片机 (型号: Leica RM 2016) 购自德国 Leica 实验技术有限公司。

1.2 尿毒症模型制备及实验动物分组 将30只SD大鼠随机分为假手术组 ($n=6$) 和实验组 ($n=24$)。24只实验组大鼠接受5/6肾切除术(Platt法)以制备慢性肾衰竭大鼠模型^[10-11], 实验组中所有大鼠在手术后均存活。手术共切除肾脏约80%。成模3周后, 大鼠接受高磷(phosphorus, P)饮食[1.2% P, 1.0% 钙(calcium, Ca)] 喂养, 制备尿毒症高转化骨病模型^[12]。术后12周, 实验组大鼠随机分为模型组、Ang(1-7)组[200 ng·kg⁻¹·min⁻¹ Ang(1-7), 通过皮下微量渗透泵输注]、DIZE组(1 mg·kg⁻¹·d⁻¹ DIZE灌胃)和A779组(400 ng·kg⁻¹·mL⁻¹ A779, 通过皮下微量渗透泵输注), 每组6只。各组大鼠于术后17周给予腹腔注射四环素1次, 采用四环素双标记法观察大鼠骨形成的动态变化。术后18周用脊髓脱臼法处死各组大鼠。

1.3 各组大鼠体质量、24 h尿蛋白(urine protein, UP)和血清生化指标检测 使用动物电子秤记录各组大鼠的体质量; 分别于术后12和18周收集各组大鼠24 h尿液, 采用尿液分析仪测定24 h UP。自大鼠内眦静脉取血0.5 mL, 经3 000 r·min⁻¹离心10 min后收集血清, 采用全自动生化分析仪测定各组大鼠血清中Ca、P、血肌酐(serum creatinine, Scr)和血尿素氮(blood urea nitrogen, BUN)水平, 采用免疫化学荧光法测定各组大鼠全段甲状旁腺素(intact parathyroid hormone, iPTH)水平。

1.4 ELISA法检测各组大鼠血清OC、NTX和TRAP-5b水平 术后12和18周, 采用ELISA法检测各组大鼠血清OC、NTX和TRAP-5b水平。

1.5 高分辨率显微CT扫描检测各组大鼠股骨组织参数 处死大鼠后取右侧股骨置于4%多聚甲醛中固定48 h, 之后用70%的乙醇浸泡, 于4℃冰箱中固定保存。取各组大鼠股骨近端骨送上海中医药大学骨伤科研究所小动物CT中心, 采用高分辨率显微CT扫描, 检测各组大鼠股骨组织参数。扫描时将标本固定在检测管中, 取距离股骨近端生长板与干骺交界处2 mm以外的长方形区域为高分辨率显微CT扫描区, 共分析2 mm, 约180层。调节显微CT参数: 电压70 kV, 电流114 μA, 分辨率为每像素10 μm。完成扫描后, 使用高分辨率231Micro VIVA-CT80系统分析各组大鼠骨密度(bone mineral density, BMD)、组织矿物质密度(tissue mineral density, TMD)、骨小梁厚度

(trabecular thickness, Tb. Th)和骨小梁分离度(trabecular separation, Tb. Sp)等三维结构参数^[13]。

1.6 Von Kossa染色和吉姆萨染色观察各组大鼠皮质骨及骨小梁病理形态表现 处死大鼠后, 取左侧股骨包埋后制成塑料块, 用轮转式切片机制片, 厚度约为7 μm, 行Von Kossa染色和吉姆萨染色后封片, 采用全自动图像数字化分析仪对每组大鼠骨组织切片进行测量, 光学显微镜下观察各组大鼠皮质骨和骨小梁病理形态表现, 计算骨小梁体积(trabecular bone volume, TBV); 荧光显微镜下测量骨形成动态参数骨矿化率(mineral apposition rate, MAR)。使用甲苯胺蓝染色辅以固绿复染进行成骨细胞计数, 用TRAP进行破骨细胞染色并计数, 计算成骨细胞指数(osteoblast index, OBI)和破骨细胞指数(osteoclast index, OCI)^[14]。

1.7 统计学分析 采用SPSS 20.0统计软件进行统计学分析。各组大鼠体质量、24 h UP, 血清中Scr、BUN、iPTH、Ca和P水平, 血清OC、NTX和TRAP水平, 股骨BMD、TMD、Tb. Th和Tb. Sp, TBV、MAR、OBI和OCI均符合正态分布, 以 $\bar{x} \pm s$ 表示, 多组间样本均数比较采用单因素方差分析, 组间样本均数两两比较采用LSD-*t*检验, 同组不同时间点样本均数比较采用配对样本*t*检验。以 $P < 0.05$ 为差异有统计学意义。

2 结果

2.1 术后12和18周各组大鼠体质量、24 h UP、Scr和BUN水平 术后12和18周, 与假手术组比较, 模型组、Ang(1-7)组、DIZE组和A779组大鼠体质量减小($P < 0.05$); 与术后12周比较, 术后18周模型组、Ang(1-7)组、DIZE组和A779组大鼠体质量差异无统计学意义($P > 0.05$)。术后12和18周, 与假手术组比较, 模型组、Ang(1-7)组、DIZE组和A779组大鼠血清中24 h UP、Scr及BUN水平均升高($P < 0.05$), 证实慢性肾衰竭大鼠模型构建成功; 术后18周, 模型组、Ang(1-7)组、DIZE组和A779组大鼠上述指标升高更加明显($P < 0.05$); 术后18周, 与模型组比较, Ang(1-7)组和DIZE组大鼠血清中24 h UP及Scr水平均降低($P < 0.05$), A779组大鼠血清中24 h UP、Scr和BUN水平均升高($P < 0.05$), 证实A779组大鼠肾损害程度最严重。见表1。

2.2 术后12和18周各组大鼠血清中iPTH、Ca及P水平 术后12和18周, 假手术组大鼠血清中iPTH、

Ca和P水平均保持在正常范围内;与假手术组比较,模型组、Ang(1-7)组、DIZE组和A779组大鼠血清中iPTH及P水平均明显升高($P<0.05$)。与术后12周比较,术后18周模型组和Ang(1-7)组大鼠血清中iPTH水平均升高($P<0.05$),A779组

大鼠血清中iPTH和P水平均升高($P<0.05$)。术后18周,与模型组比较,A779组大鼠血清中iPTH和P水平均升高($P<0.05$);与模型组比较,Ang(1-7)组和DIZE组大鼠血清中iPTH及P水平差异均无统计学意义($P>0.05$)。见表2。

表1 术后12和18周各组大鼠血清中24 h UP、Scr及BUN水平

Tab. 1 Levels of 24 h UP, Scr, and BUN in serum of rats in various groups at 12 and 18 weeks after operation ($n=6, \bar{x} \pm s$)

Group	Body weight(m/g)		24 h UP(mg·d ⁻¹)		Scr[c _B /(μmol·L ⁻¹)]		BUN[c _B /(mmol·L ⁻¹)]	
	(week)12	18	12	18	12	18	12	18
Sham operation	156±12	149±17	8±1	7±2	66±34	69±36	5±1	6±1
Model	128±21*	119±25*	52±12*	67±29*#	94±12*	170±37*#	15±3*	26±7*#
Ang(1-7)	122±27*	118±16*	58±18*	60±26* [△]	92±21*	110±27* [△]	16±1*	18±5* [△] #
DIZE	115±22*	121±18*	48±15*	62±14* [△] #	97±26*	116±35* [△]	16±5*	22±7* [△] #
A779	112±25*	114±23*	62±10*	74±25* [△] #	99±17*	230±32* [△] #	17±2*	29±11* [△] #

* $P<0.05$ vs sham operation group; [△] $P<0.05$ vs model group; # $P<0.05$ vs 12 weeks after operation.

表2 术后12和18周各组大鼠血清中iPTH、Ca及P水平

Tab. 2 Levels of iPTH, Ca, and P in serum of rats in various groups at 12 and 18 weeks after operation ($n=6, \bar{x} \pm s$)

Group	iPTH[c _B /(pmol·L ⁻¹)]		Ca[c _B /(mmol·L ⁻¹)]		P[c _B /(mmol·L ⁻¹)]	
	(week)12	18	12	18	12	18
Sham operation	35±7	34±12	2.3±0.3	2.3±0.1	1.3±0.1	1.3±0.1
Model	67±21*	102±16*#	2.4±0.1	2.3±0.2	2.6±0.1*	2.6±0.4*
Ang(1-7)	70±21*	95±20*#	2.2±0.2	2.3±0.1	2.2±0.5*	2.3±0.2*
DIZE	66±19*	101±32*	2.2±0.3	2.3±0.2	2.5±0.2*	2.6±0.1*
A779	76±24*	108±21* [△] #	2.4±0.3	2.4±0.1	2.5±0.1*	2.8±0.5* [△] #

* $P<0.05$ vs sham operation group; [△] $P<0.05$ vs model group; # $P<0.05$ vs 12 weeks after operation.

2.3 术后12和18周各组大鼠血清中OC、NTX及TRAP-5b水平 假手术组大鼠血清中OC、NTX和TRAP-5b骨代谢指标均处于正常范围。术后12和18周,与假手术组比较,模型组、Ang(1-7)组、DIZE组和A779组大鼠血清中OC、NTX及TRAP-5b水平均升高($P<0.05$);与术后12周比较,术后18周模型组大鼠血清中NTX水平升高

($P<0.05$),A779组大鼠血清中NTX和TRAP-5b水平升高($P<0.05$);术后12周,与模型组比较,Ang(1-7)组、DIZE组和A779组大鼠血清中TRAP-5b水平均降低($P<0.05$);术后18周,与模型组比较,Ang(1-7)组和DIZE组大鼠血清中NTX及TRAP-5b水平均降低($P<0.05$),A779组大鼠血清中NTX和TRAP-5b水平升高($P<0.05$)。见表3。

表3 术后12和18周各组大鼠血清OC、NTX及TRAP-5b水平

Tab. 3 Levels of serum OC, NTX, and TRAP-5b of rats in various groups at 12 and 18 weeks after operation ($n=6, \bar{x} \pm s$)

Group	OC [ρ _B /(μg·L ⁻¹)]		NTX [c _B /(nmol·L ⁻¹)]		TRAP-5b [λ _B /(U·L ⁻¹)]	
	(week) 12	18	12	18	12	18
Sham operation	1.3±0.1	1.4±0.1	33±12	36±16	3.6±0.4	5.4±1.9
Model	2.1±0.3*	2.4±0.3*	89±22*	111±25*#	10.4±1.1*	10.6±1.2*
Ang(1-7)	2.3±0.3*	2.3±0.3*	83±17*	85±31* [△]	8.4±0.3* [△]	8.3±0.7* [△]
DIZE	2.2±0.1*	2.3±0.2*	96±19*	98±11* [△]	8.2±3.3* [△]	8.5±1.2* [△]
A779	2.3±0.3*	2.3±0.3*	85±16*	128±29* [△] #	10.0±1.7* [△]	12.4±3.6* [△] #

* $P<0.05$ vs sham operation group; [△] $P<0.05$ vs model group; # $P<0.05$ vs 12 weeks after operation.

2.4 各组大鼠股骨BMD、TMD、Tb.Th和Tb.Sp

与假手术组比较, 模型组、Ang(1-7)组、DIZE组和A779组大鼠股骨近端区域骨小梁的BMD和TMD均降低 ($P<0.05$); 与模型组比较, Ang(1-7)组和DIZE组大鼠股骨BMD及TMD升高 ($P<0.05$), A779组大鼠股骨BMD和TMD降低 ($P<0.05$)。与假手术组比较, 模型组大鼠股骨近端Tb.Th降低 ($P<0.05$), Tb.Sp升高 ($P<0.05$), Ang(1-7)组和DIZE组大鼠股骨近

端Tb.Th升高 ($P<0.05$), 而Tb.Sp降低 ($P<0.05$); 与模型组比较, A779组大鼠股骨近端Tb.Th降低 ($P<0.05$), 而Tb.Sp升高 ($P<0.05$)。见表4。

2.5 各组大鼠骨小梁病理形态表现 Von Kossa染色结果显示: 与假手术组比较, 模型组大鼠骨小梁数量明显减少; 与模型组比较, Ang(1-7)组和DIZE组大鼠骨小梁数量明显增加, A779组大鼠骨小梁数量减少。见图1。

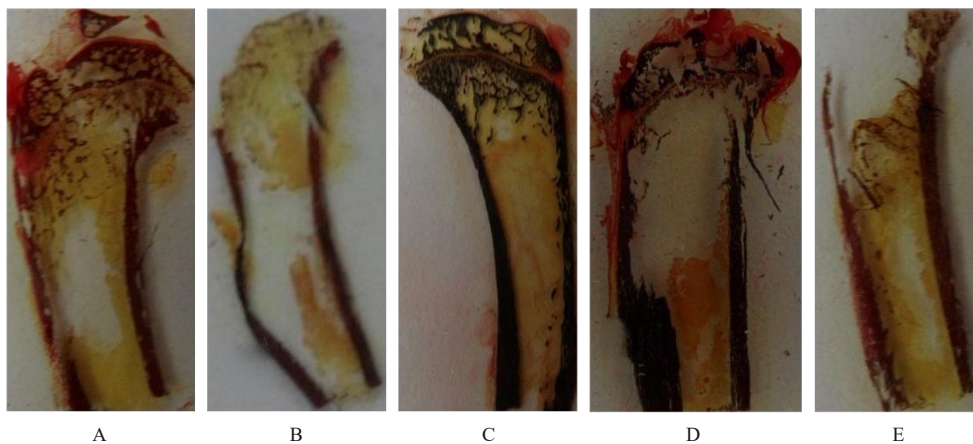
表4 各组大鼠股骨BMD、TMD、Tb.Th和Tb.Sp

Tab. 4 BMD, TMD, Tb. Th, and Tb. Sp in femur of rats in various groups

($n=6, \bar{x}\pm s$)

Group	BMD($\text{g}\cdot\text{cm}^{-3}$)	TMD($\text{mgHA}\cdot\text{cm}^{-3}$)	Tb.Th($l/\mu\text{m}$)	Tb.Sp($l/\mu\text{m}$)
Sham operation	210±82	891±125	7.6±1.2	6.5±1.2
Model	101±32*	320±128*	3.9±0.3*	11.3±2.3*
Ang(1-7)	189±72 [△]	710±201 [△]	5.5±2.1 [△]	6.5±1.0 [△]
DIZE	185±56 [△]	810±138 [△]	5.9±2.0 [△]	7.5±1.0 [△]
A779	62±10 [△]	271±22 [△]	3.1±1.0 [△]	13.5±1.0 [△]

* $P<0.05$ vs sham operation group; [△] $P<0.05$ vs model group.



A: Sham operation group; B: Model group; C: Ang(1-7) group; D: DIZE group; E: A779 group.

图1 各组大鼠皮质骨和骨小梁大体病理形态表现(Von Kossa, ×4)

Fig. 1 Pathomorphology of cortical and trabecular bone of rats in various groups(Von Kossa, ×4)

2.6 各组大鼠股骨TBV、MAR、OBI和OCI 与假手术组比较, 模型组、Ang(1-7)组、DIZE组和A779组大鼠股骨TBV降低 ($P<0.05$); 与模型组比较, Ang(1-7)组和DIZE组大鼠股骨TBV略升高 ($P<0.05$), 而A779组大鼠股骨TBV降低 ($P<0.05$)。荧光显微镜检查结果显示: 与假手术组比较, 模型组、Ang(1-7)组、DIZE组和A779组大鼠股骨MAR升高 ($P<0.05$); 光学显微镜检查结果显示: 与模型组比较, Ang(1-7)组和DIZE组大鼠股骨OCI及OBI降低 ($P<0.05$),

而A779组大鼠股骨OBI和OCI升高 ($P<0.05$)。见表5。

3 讨论

近年来, 随着血液净化技术的持续提升, 尿毒症患者的透析年限逐步延长, CKD-MBD的发病率呈现逐年递增的趋势^[15]。由继发性甲状旁腺功能亢进症 (secondary hyperparathyroidism, SHPT) 引发的骨骼合成与分解代谢失衡, 临床表现为骨质疏松、骨关节疼痛和自发骨折等症状^[16]; 血管钙

表5 各组大鼠股骨组织TBV、MAR、OBI和OCI

Tab. 5 TBV, MAR, OBI, and OCI in femur tissue of rats in various groups ($n=6, \bar{x} \pm s$)

Group	TBV ($\eta/\%$)	MAR ($\mu\text{m}\cdot\text{d}^{-1}$)	OBI ($\eta/\%$)	OCI ($\eta/\%$)
Sham operation	8.0±3.2	1.9±0.6	17.5±6.1	8.1±2.1
Model	6.6±1.2*	5.3±2.1*	25.1±5.4*	14.3±4.4*
Ang(1-7)	7.0±2.1 [△]	5.7±3.8*	20.8±5.0 [△]	9.1±2.7 [△]
DIZE	7.3±2.2 [△]	5.2±1.9*	18.2±3.9 [△]	9.2±3.3 [△]
A779	6.1±1.3 [△]	5.9±0.1*	35.5±6.1 [△]	23.1±8.1 [△]

* $P<0.05$ vs sham operation group; [△] $P<0.05$ vs model group.

化已成为尿毒症患者主要不良心脏事件和全因死亡率的独立危险因素^[17-18]。骨组织RAS的发现为治疗CKD-MBD和SHPT提供了新的研究方向及思路^[19]。本研究采用5/6肾切除法并结合高P饮食喂养24只实验组大鼠,结果表明:在术后12周,实验组大鼠24h UP、Scr和BUN水平均升高,证实了慢性肾衰竭大鼠模型的成功构建。同时,与假手术组比较,实验组大鼠血清iPTH、P、OC、NTX和TRAP-5b水平均升高;高分辨率显微CT扫描检测结果显示实验组大鼠骨小梁BMD降低,骨量减少,TBV降低;骨病理检查结果证实实验组大鼠OBI和OCI升高,与高转化骨病的骨病理特征相符^[11, 20],表明尿毒症高转化骨病大鼠模型的成功制备。

OC、NTX和TRAP-5b是与骨代谢存在密切相关的重要指标^[21]。本研究结果显示:与假手术组比较,实验组大鼠血清中OC、NTX和TRAP-5b水平均明显升高,提示实验组大鼠的成骨细胞和破骨细胞活性均有所增加,骨代谢的速度也随之提升。给予Ang(1-7)和DIZE后,与模型组比较,Ang(1-7)组和DIZE组大鼠血清OC、NTX和TRAP-5b水平均降低,提示Ang(1-7)和DIZE均可使破骨细胞活性降低,从而缓解高转化骨病的骨吸收现象。使用Mas受体拮抗剂A779进行干预时,A779组大鼠的破骨细胞活性增强,骨破坏现象更为严重。

本研究高分辨率显微CT扫描检测结果显示:Ang(1-7)和DIZE能提升Ang(1-7)组及DIZE组大鼠的Tb.Th,降低Tb.Sp,对高分解代谢引发的骨骼破坏具有缓解作用,并积极抑制BMD降低。

各组大鼠股骨计量学参数检测结果显示:模型组大鼠股骨形态发生改变,表现为骨小梁结构紊乱,骨细胞减少。而Ang(1-7)组和DIZE组大鼠的股骨组织学形态改善,骨小梁结构较为规整,骨细胞数量增加。上述结果进一步证实了Ang(1-7)和DIZE通过调节大鼠骨组织中成骨细胞及破骨细胞的活性,促进骨形成,抑制骨吸收,从而改善模型组大鼠的骨代谢状况。这一结果与血清中骨吸收和骨形成标志物OC、NTX及TRAP的变化相吻合。ACE2激动剂DIZE与Mas拮抗剂A779通过对Ang(1-7)和Mas受体的双重调控,结果提示:ACE2/Ang(1-7)/Mas轴在尿毒症高转化骨病中骨代谢失衡的发生发展过程中具有重要作用。Ang(1-7)抑制破骨细胞分化^[22-23],促进成骨细胞增殖^[24],从而提高骨的形成。这种双重作用使得骨代谢保持平衡^[25]。

综上所述,ACE2激活剂DIZE能够增强Ang(1-7)的作用,进一步改善骨代谢失衡,ACE2/Ang(1-7)/Mas轴对尿毒症大鼠高转化骨病具有改善作用。本研究为尿毒症大鼠高转化骨病的治疗提供了新的思路和治疗方法。

利益冲突声明:

所有作者声明不存在利益冲突。

作者贡献声明:

薛杨参与论文撰写,阮颖新参与论文的统计学分析,闫铁昆和贾俊亚参与实验整体设计,林珊参与论文审阅和修改。

[参考文献]

- [1] 朱家恺. 外科学辞典[M]. 北京:北京科学技术出版社, 2003.
- [2] KANEKO K, ITO M, FUMOTO T, et al. Physiological function of the angiotensin AT1a receptor in bone remodeling[J]. J Bone Miner Res, 2011, 26(12): 2959-2966.
- [3] SPERETTA G F, RUCHAYA P J, DELBIN M A, et al. Importance of AT1 and AT2 receptors in the nucleus of the solitary tract in cardiovascular responses induced by a high-fat diet[J]. Hypertens Res, 2019, 42(4): 439-449.
- [4] 黎秀芝,尹新华. ACE2/Ang(1-7)/Mas轴在心血管疾病中的研究进展[J]. 医学综述, 2020, 26(20): 3969-3975.
- [5] BAYOMY O, ZAHEER S, WILLIAMS J S, et al. Disentangling the relationships between the renin-angiotensin-aldosterone system, calcium physiology,

- and risk for kidney stones[J]. *J Clin Endocrinol Metab*, 2020, 105(6): 1937-1946.
- [6] HATTON R, STIMPEL M, CHAMBERS T J. Angiotensin II is generated from angiotensin I by bone cells and stimulates osteoclastic bone resorption in vitro[J]. *J Endocrinol*, 1997, 152(1): 5-10.
- [7] 樊长萍, 侯建明. 原发性醛固酮增多症与骨质疏松症的相关性[J]. *中华骨质疏松和骨矿盐疾病杂志*, 2016, 9(2): 199-204.
- [8] SALAM S, GALLAGHER O, HUGHES D, et al. The role of static bone histomorphometry in diagnosing renal osteodystrophy[J]. *Bone*, 2021, 142: 115689.
- [9] FERREIRA A C, COHEN-SOLAL M, D'HAESE P C, et al. The Role of Bone Biopsy in the Management of CKD-MBD[J]. *Calcif Tissue Int*, 2021, 108(4): 528-538.
- [10] JØRGENSEN H S, BEHETS G, VIAENE L, et al. Static histomorphometry allows for a diagnosis of bone turnover in renal osteodystrophy in the absence of tetracycline labels[J]. *Bone*, 2021, 152: 116066.
- [11] 李红芬, 林 珊, 贾俊亚, 等. 长期低剂量 $1\alpha, 25$ -二羟基维生素D3对尿毒症大鼠肾脏水通道蛋白2表达的影响[J]. *中华肾脏病杂志*, 2013, 29(2): 124-128.
- [12] 祝再然, 林 珊, 贾俊亚, 等. 长期接受不同饮食磷水平的慢性肾衰竭大鼠骨组织形态学特征改变[J]. *北京医学*, 2011, 33(2): 167-169.
- [13] PAZIANAS M, MILLER P D. Osteoporosis and chronic kidney disease-mineral and bone disorder (CKD-MBD): back to basics[J]. *Am J Kidney Dis*, 2021, 78(4): 582-589.
- [14] TSUJI K, KITAMURA M, CHIBA K, et al. Comparison of bone microstructures via high-resolution peripheral quantitative computed tomography in patients with different stages of chronic kidney disease before and after starting hemodialysis[J]. *Ren Fail*, 2022, 44(1): 381-391.
- [15] NEYRA J A, HU M C, MOE O W. Klotho in clinical nephrology: diagnostic and therapeutic implications[J]. *Clin J Am Soc Nephrol*, 2020, 16(1): 162-176.
- [16] SAAR-KOVROV V, DONNERS M M P C, VAN DER VORST E P C. Shedding of klotho: functional implications in chronic kidney disease and associated vascular disease[J]. *Front Cardiovasc Med*, 2021, 7: 617842.
- [17] 程 虹. 中晚期慢性肾脏病患者血管钙化管理[J]. *中国实用内科杂志*, 2023, 43(3): 218-224.
- [18] 汤 曦, 石运莹, 王俭勤, 等. 中国成人慢性肾脏病及其并发症早期筛查临床路径专家建议(2023版)[J]. *中国实用内科杂志*, 2023, 43(3): 198-205.
- [19] KONO K, FUJII H, WATANABE K. Relationship between parathyroid hormone and renin-angiotensin-aldosterone system in hemodialysis patients with secondary hyperparathyroidism[J]. *J Bone Miner Metab*, 2021, 39(2): 230-236.
- [20] WANG Y L, MA W X, PU J H, et al. Interrelationships between sarcopenia, bone turnover markers and low bone mineral density in patients on hemodialysis[J]. *Ren Fail*, 2023, 45(1): 2200846.
- [21] PARK S Y, AHN S H, YOO J I, et al. Position statement on the use of bone turnover markers for osteoporosis treatment[J]. *J Bone Metab*, 2019, 26(4): 213-224.
- [22] WU J, WANG M, GUO M, et al. Angiotensin receptor blocker is associated with a lower fracture risk: an updated systematic review and meta-analysis[J]. *Int J Clin Pract*, 2022, 2022: 7581110.
- [23] QUEIROZ-JUNIOR C M, SANTOS A C P M, GALVÃO I, et al. The angiotensin converting enzyme 2/angiotensin-(1-7)/Mas Receptor axis as a key player in alveolar bone remodeling[J]. *Bone*, 2019, 128: 115041.
- [24] 章海涛. 新型盐皮质激素受体拮抗剂的临床应用[J]. *肾脏病与透析肾移植杂志*, 2021, 30(5): 449-450.
- [25] TIWARI P, TIWARI V, GUPTA S, et al. Activation of angiotensin-converting enzyme 2 protects against lipopolysaccharide-induced glial activation by modulating angiotensin-converting enzyme 2/angiotensin (1-7)/mas receptor axis[J]. *Mol Neurobiol*, 2023, 60(1): 203-227.